Materials Science and Engineering A 409 (2005) 317–328

www.elsevier.com/locate/msea

Influence of titanium oxide films on copper nucleation during electrodeposition

Hyun K. Chang [a], Byung-Hak Choe [b], Jong K. Lee [c,*]

[a] *School of Metallurgical and Materials Engineering, Sung Kyun Kwan University, Suwon 440-746, South Korea*
[b] *Department of Metallurgical Engineering, Kangnung National University, Kangnung 210-702, South Korea*
[c] *Department of Materials Science & Engineering, Michigan Technological University, Houghton, MI 49931, USA*

Received in revised form 15 March 2005; accepted 18 March 2005

Abstract

Copper electrodeposition has an important industrial role because of various interconnects used in electronic devices such as printed wire boards. With an increasing trend in device miniaturization, in demand are void-free, thin copper foils of 10 μm thick or less with a very low surface profile. In accordance, nucleation kinetics of copper was studied with titanium cathodes that were covered with thin, passive oxide films of 2–3 nm. Such an insulating oxide layer with a band gap of 3 eV is supposed to nearly block charge transfer from the cathode to the electrolyte. However, significant nucleation rates of copper were observed. Pipe tunneling mechanism along a dislocation core is reasoned to account for the high nucleation kinetics. A dislocation core is proposed to be a high electron tunneling path with a reduced energy barrier and a reduced barrier thickness. In supporting the pipe tunneling mechanism, both 'in situ' and 'ex situ' scratch tests were performed to introduce extra dislocations into the cathode surface, that is, more high charge paths via tunneling, before electrodeposition.

Keywords: Electrodeposition; Titanium cathode; Copper nucleation; Dislocation; Titanium oxide; Pipe tunnelling; Anodization

1. Introduction

Copper foils for printed wire boards are usually laminated to a substrate of synthetic resin such as epoxy, and then printed with the pattern of a desired circuit before unwanted portions are etched away. With an increasing trend in device miniaturization, both electronic and battery industry require void-free foils of 10 μm thick or less with a very low surface profile, that is, a uniform thickness. Such copper foils are produced through electrodeposition with cathode drums of about 2 m diameter and 2 m wide. From a materials science viewpoint, foil production is an interesting challenge as a thin, uniform foil of 2 m wide and 100 m long demands well-controlled nucleation and growth of copper on the cathode surface. Additionally, the finished copper foil should be readily separable from the rotating cathode drum surface, which returns for a new foil production process. Based on experience, titanium has been widely adopted as a cathode in copper foil industry. In this work, nucleation kinetics of copper on a titanium cathode was studied in a hope to shed some light for better foil production.

Electrodeposition of copper from electrolytes such as acid copper sulfate solutions is extensively used for electroforming, electrorefining and electroplating. Accordingly, numerous investigations have been carried out to address mechanical and physical properties of copper deposits, optimum conditions of operating temperature, current density and electrolyte concentration, effects of additives, etc. [1–7]. In this work, we will focus on the role of a passive oxide layer naturally forming on a titanium surface in ambient air. In Section 2, experimental procedures are outlined. Section 3 presents the results. The first part addresses both 'in situ' and 'ex situ' scratch tests, which

* Corresponding author. Tel.: +1 906 487 2266; fax: +1 906 487 2934.
E-mail address: jkl103@mtu.edu (J.K. Lee).

0921-5093/$ – see front matter © 2005 Elsevier B.V. All rights reserved.
doi:10.1016/j.msea.2005.03.114

become a basis for the proposed pipe tunneling mechanism. Results for cathode surface modification are then followed. Finally, discussion and conclusion are presented in Sections 4 and 5, respectively. It is noted that some of the preliminary results were published in conference proceedings [8,9].

2. Experimental procedure

The electrolyte was prepared from Fisher certified grade cupric sulfate pentahydrate and reagent grade sulfuric acid to give a stock electrolyte with a concentration of 100 g/l copper and 100 g/l sulfuric acid. Cathodes were made of 32 μm thick titanium foils with 99.7% purity from Alfa Aesar, which were hot-rolled, annealed and then pickled in an acid before shipping. The electrolytic cell was a water-jacketed glass beaker, which allowed for the electrolyte temperature to be maintained at 65 °C. The reference electrode was a mercury/mercurous sulfate electrode and a copper plate was used as the counter electrode. Deposition was administered through an EG&G Model 273. Copper plating was performed in a galvanostatic mode at the current densities ranging from 100 to 500 mA/cm^2. To closely probe copper nucleation, the currents less than industrial values (600–1200 mA/cm^2) were employed. Structural characterization of copper deposits was examined ex situ by scanning electron microscopy (SEM) with a JSM-6400.

3. Results

3.1. Scratch test

In copper foil industry for printed wire boards, electrodeposition is typically performed at an electric current of 600 mA/cm^2 or higher with addition of small amounts of organic agents. In this work, however, electrodeposition was carried out at low currents in order to better analyze copper nucleation at slow kinetics. Some results are shown in Fig. 1. The top row shows the morphologies of copper clusters obtained at the current densities of Fig. 1a 200 and Fig. 1b 500 mA/cm^2 for 1 s. All the images represent electrodeposition at an additive-free condition. Consistent with the results of other investigations [1,2], the effect of the current density is clear, even for deposition of only 1 s. Clusters became finer and more copious with an increase in the current density: for example, the cluster density shows a change from $\sim 3 \times 10^6$ cm^{-2} at 200 mA/cm^2 to $\sim 4 \times 10^7$ cm^{-2} at 500 mA/cm^2. Even if one accounts for smaller average cluster size at 500 mA/cm^2, the density increase by an order of 10, much greater than the current ratio of 2.5, suggests that

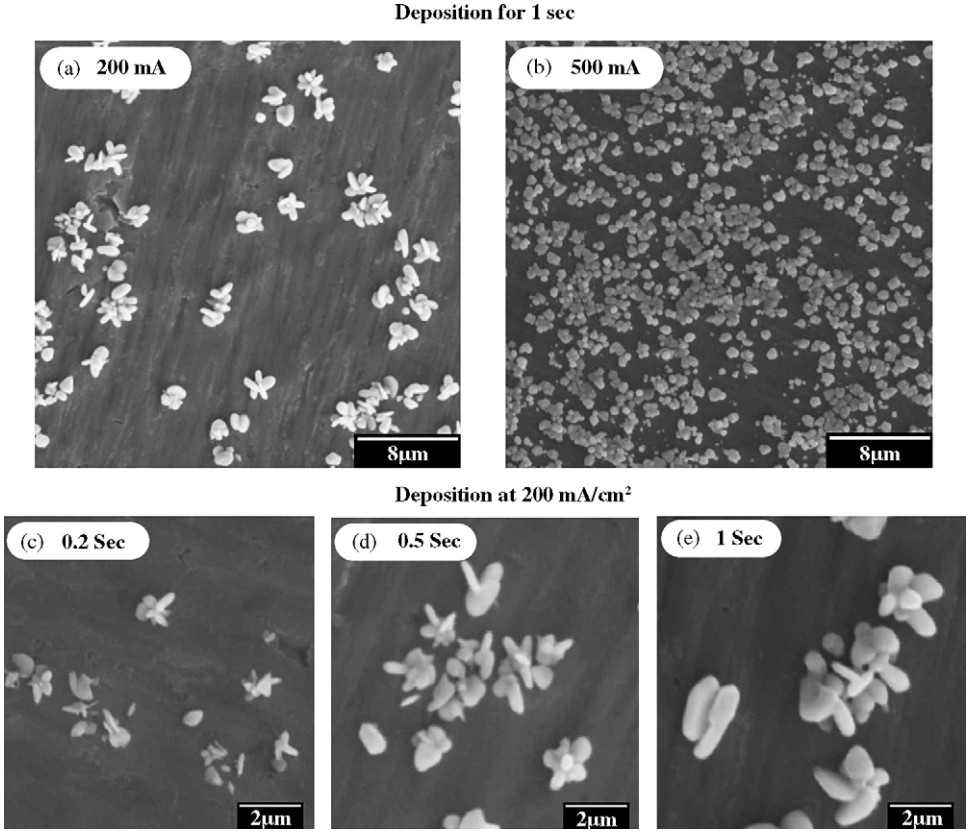

Fig. 1. Comparison of copper cluster morphologies. The upper row of (a) and (b) shows clusters obtained at 200 and 500 mA/cm^2 for 1 s. The lower row displays clusters obtained at 200 mA/cm^2 for (c) 0.2, (d) 0.5 and (e) 1 s, respectively.

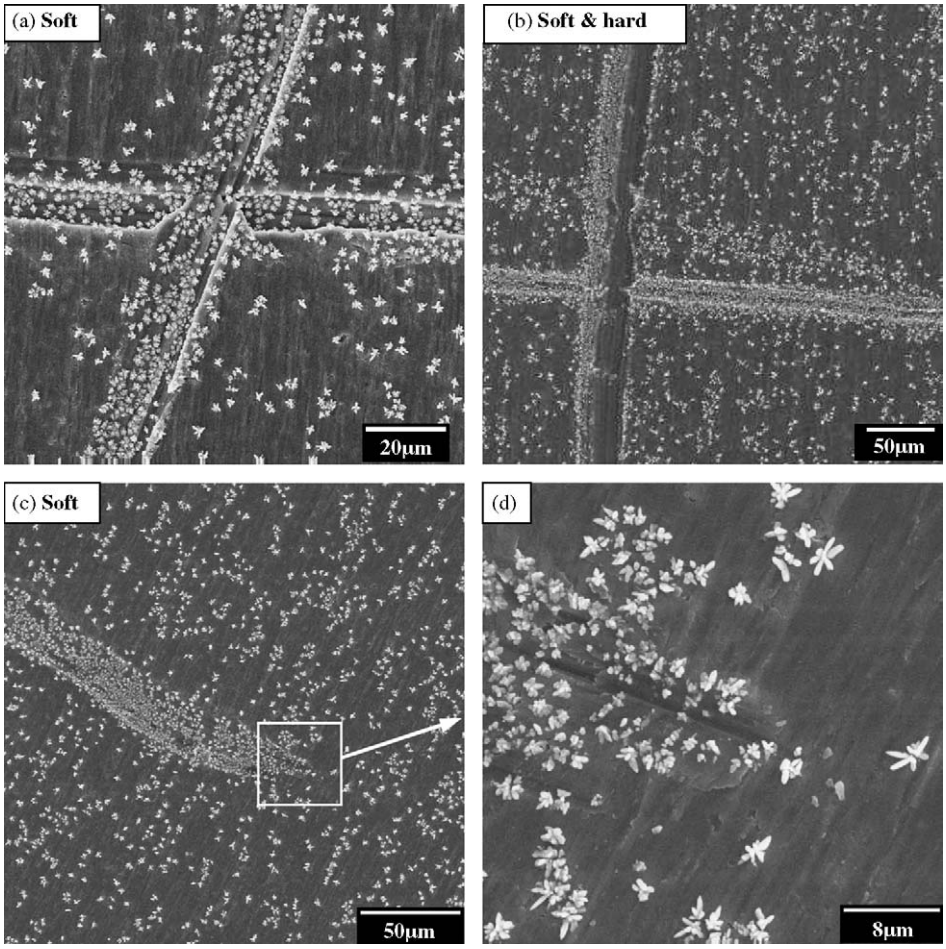

Fig. 2. Copper clusters along 'in situ' scratch marks. (a) Shows copious copper clusters at two crisscrossing soft scratches, (b) contrasts a horizontal, soft scratch line against a vertical, hard scratch mark, (c) demonstrates another soft scratch line and whose tail end is shown in (d) at a higher magnification. All were at 200 mA/cm^2 for 1 s.

the deposition kinetics at 200 mA/cm^2 was quite sluggish. At 200 mA/cm^2, the cluster size is almost uniform, indicating that its nucleation kinetics was somewhat instantaneous. On the other hand, the size distribution at 500 mA/cm^2 displays small as well as large particles, and thus the kinetics should have developed progressively. Later, we will further discuss the effect of a higher current density. The images at 200 mA/cm^2 also reveal that copper nucleation was neither random and its growth was nor epitaxial. In order to examine early-stage cluster formation, images at 0.2, 0.5 and 1 s, all at 200 mA/cm^2, are also displayed in Fig. 1. Clearly, copper nucleation occurred very selectively, hinting preferential nucleation sites.

Although pickled in a HNO_3/HF acid before shipping, the surface of an as-received titanium cathode was known to have a passive oxide layer of about 2–3 nm thick [10]. Presence of such a thin oxide layer can be detected through an X-ray photoelectron spectroscope [11]. In this work, however, two rudimentary approaches were employed to see the role of the oxide layer in copper nucleation. In 'in situ scratch tests', the cathode surface was, while immersed in the electrolytic cell, scratched with a razor blade thus avoiding exposure to oxygen atmosphere, and then electrodeposition was carried out. In order to control the amount of scratch force, an MTS-XP nano-indenter was employed in 'ex situ scratch tests.' In the latter tests, the cathode surface was fully exposed to air before electrodeposition.

In Fig. 2, Cu clusters are probed along both 'soft' and 'hard' in situ scratch marks. A soft scratch means a shallow mark about 10 μm wide or less, while a wider and deeper mark is termed a hard scratch. In Fig. 2a, copious copper clusters are shown along two crisscrossing soft scratch lines. In Fig. 2b, extensive clusters are shown along the horizontal, soft scratch line. Along the vertical, hard scratch line, however, both cluster-free and cluster-full bands are shown to run side by side. In Fig. 2c, numerous nucleation is evidenced along a soft scratch mark and Fig. 2d shows the tail portion of the scratch line at a higher magnification. All the depositions were performed at 200 mA/cm^2.

Scratching inflicted both plastic deformation and fracture, among others, on the cathode surface [12]. When it was sufficiently intense, the TiO_2 layer should have been plowed away, exposing a bare Ti surface to the electrolyte. Thus, the central region of a scratch track became oxide-free and acted

as a highly potential site for copper nucleation. It is why soft scratch lines were covered with numerous copper clusters. On the other hand, when a scratch process created too deep a groove, its central region of a deep groove became less favorable for copper nucleation because of the point effects of charge distribution. It can be reasoned why the trace of the vertical, hard scratch line of Fig. 2b shows practically a cluster-free zone. During scratching, both debris and scales, plowed away from the central region, were stacked at the side banks. In addition, numerous dislocations were generated in the bank region through extensive plastic deformation. Dislocation generation during scratching was well documented in the literature for dislocation mobility measurement experiments [13,14]. Therefore, it seems reasonable to conjecture

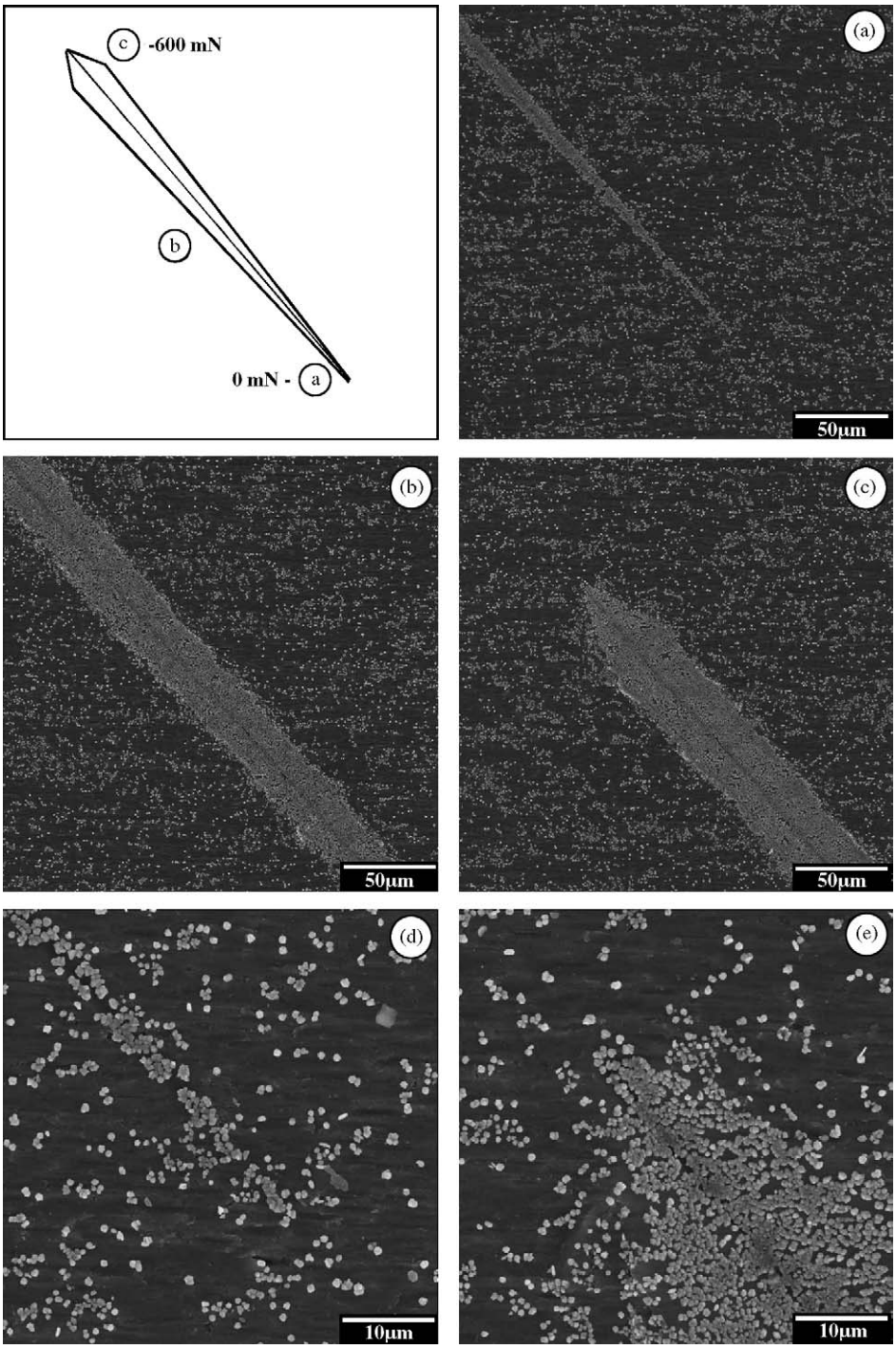

Fig. 3. Enhanced copper cluster density along an 'ex situ' scratch line. Through an MTS-XP nano-indenter, a 1 mm scratch line was created from zero force at the point marked with (a) to a force of 600 mN at the end marked with (c). (b) Indicates the middle point. The images of (d) and (e) are enlarged ones for (a) and (c), respectively.

that the copious clusters shown on the left bank of the vertical scratch line are a direct result of abundant dislocations produced there. Why fewer or almost no copper clusters on the right bank? Some are shown, but they are hardly comparable to those on the left side. Because of unbalanced scratch forces as well as anisotropy both in crystal structure and in dislocation mobility, the dislocation distribution at an in situ scratch line was typically found to be asymmetrical [14]. Thus, an asymmetry in dislocation distribution is reasoned to have caused an asymmetry in cluster distribution. For a soft scratch, both the oxide-free surface and the dislocations were responsible for the enhanced cluster density of about 10^8 cm^{-2}, which is greater by an order of 10–100 than the density of an un-scratched cathode surface.

In order to impose balanced as well as controlled forces during scratching, an MTS-XP nano-indenter was employed to introduce ex situ scratches on the titanium cathode surfaces before electrodeposition. Fig. 3 shows enhanced copper nucleation along a 1 mm scratch line, which was formed from zero force at the point marked with a to a force of 600 mN at the end marked with c. The scratch line is sketched at the top left corner. Fig. 3a displays copper cluster distribution in the

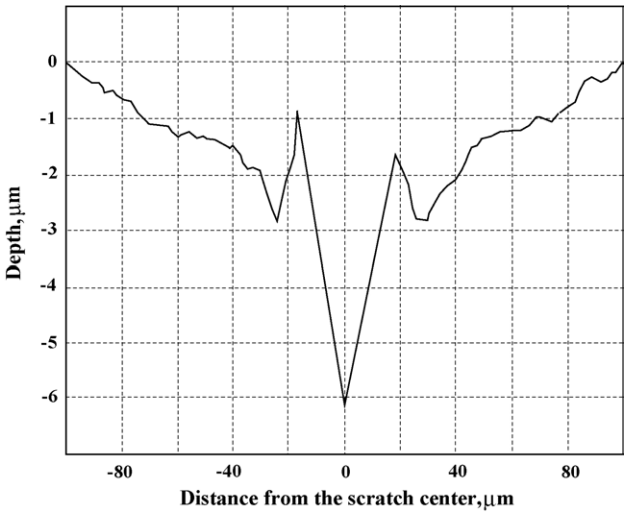

Fig. 4. A typical surface profile across an 'ex situ' scratch line which was created under a load of 600 mN. Note the banks of about 1–2 μm high on both sides of the groove.

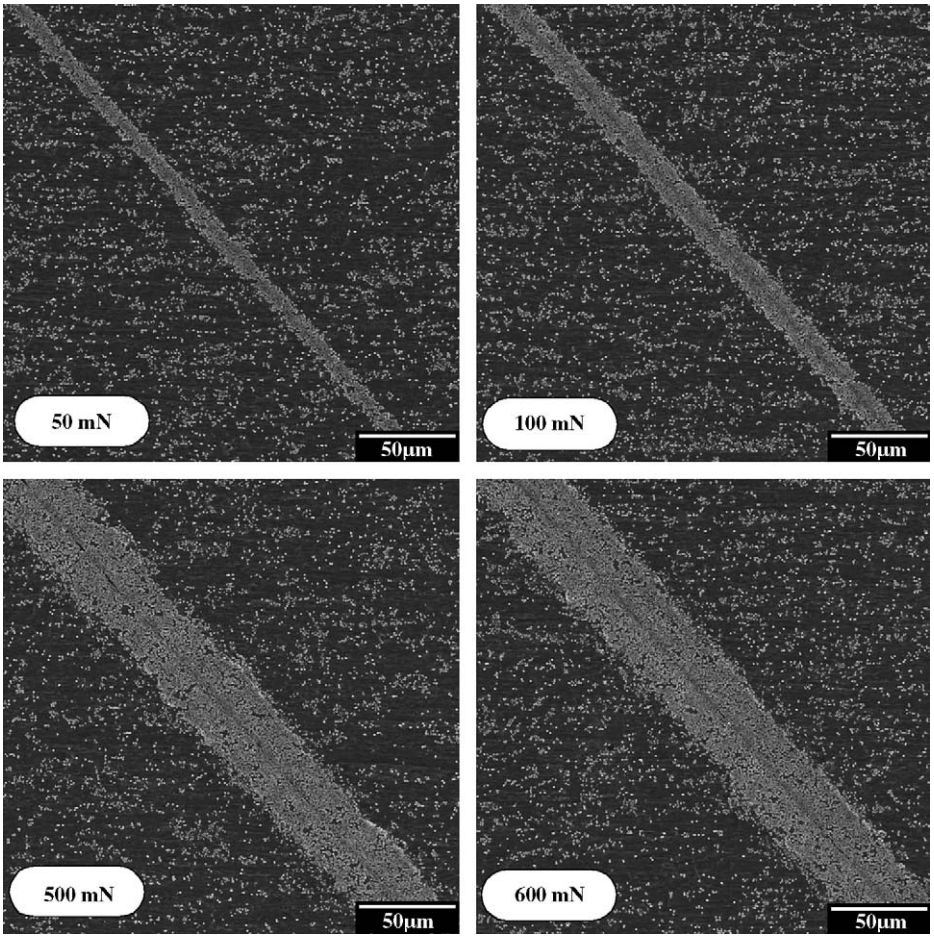

Fig. 5. Copper cluster distribution along 'ex situ' scratch lines created under constant loads: the loads were 50, 100, 500 and 600 mN.

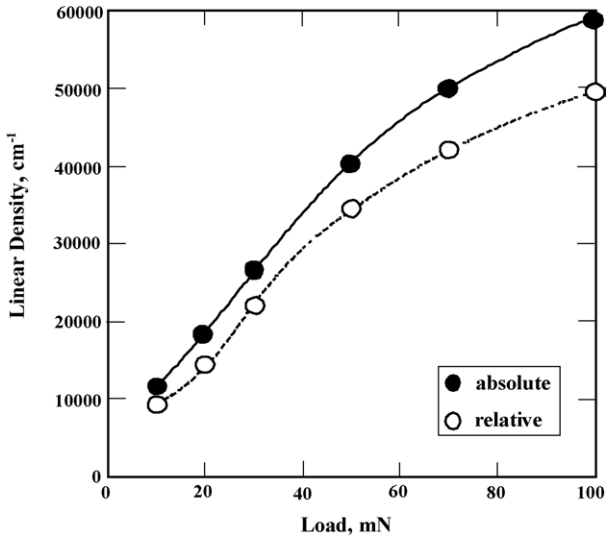

Fig. 6. Linear cluster density as a function of the scratch load. The upper curve indicates absolute counts per centimetre, while the lower one presents the value relative to that of the unscratched matrix region.

proximity of the starting point for the scratch, Fig. 3b for the midway and Fig. 3c for the end point of the scratch where the force reached 600 mN. With an increase in the indenter force, the width of the deformed region is shown to increase. The indenter was a three-side pyramidal diamond, which created a valley at the scratch center. Fig. 3d is an enlarged picture of the starting point and Fig. 3e is for the end point. Clearly, the copper cluster density is shown to be much higher along the scratch line than a unscratched matrix region. Deposition was performed under a galvanostatic condition with 100 mA/cm^2 for 1 s.

A typical surface profile across a scratch line is pictured in Fig. 4, which shows a 40 μm wide and a 5–6 μm deep groove created under the load of 600 mN. Note the banks of about 1–2 μm high on both sides of the groove. In Fig. 3, both Fig. 3b and c displayed different contrast along the scratch central line: it is a region of deep groove and also of low cluster density due to the point effect of charge distribution. For comparison to the incremental load for indentation in Fig. 3, results of constant loads are shown in Fig. 5. The scratch loads were 50, 100, 500 and 600 mN: the width increased with an increase in the load. The deposition conditions were identical to those of Fig. 3. Enhanced cluster density was examined as a function of scratch load, and is shown in Fig. 6. To manage density calculation to a reasonable accuracy, the loads were limited under 100 mN. The linear density, i.e. the number of copper clusters per centimetre along a scratch line, is given. The upper, solid curve indicates the number of copper clusters as were counted. The lower, dotted curve displays the cluster number relative to the unscratched matrix region, that is, the number of clusters in the matrix region was subtracted from the absolute number of the top curve. Clearly, scratching a cathode surface has shown a profound effect on the deposition kinetics of copper.

3.2. Pipe tunneling

Though indirect, scratch tests revealed both the presence of an oxide layer at the cathode surface and the role of dislocations in copper nucleation. A typical cluster density in an un-scratched area at a low current density of 200 mA/cm^2 is about 10^6 cm^{-2}, which is in the range of the dislocation density, 10^6–10^7 cm^{-2}, for an annealed metal. This also manifests that dislocations are crucial in copper nucleation on the titanium cathode surface covered with an oxide layer. Therefore, it seems reasonable to further examine the nature of the oxide layer as well as the charge transfer through a dislocation line. Although a troublemaker for copper nucleation, the oxide layer itself, oddly, provides both copper foil and bio-materials industries with beneficial effects: it promotes easy separation between the cathode and the finished copper foil at the end of electrodeposition process, and good bio-compatibility through strong cell adhesion as part of an implantable device.

Titanium oxides provides rich polymorphism. For TiO_2, there are rutile (tetragonal), anatase (tetragonal) and brookite (orthorhombic) [15]. In addition, a variety of structures are reported for Ti_nO_{2n-1}, which includes TiO. For the annealed and pickled titanium cathodes used in the present work, it may be reasonable to assume that the oxide was the most stable structure, rutile with a band energy gap equal to 3 eV. Because of the thickness with only 2–3 nm, a TEM work was not attempted. Fortunately, Tanaka reported an excellent TEM work on the interface between Ti and about 10 nm rutile crystallite [16]. His work shows that a hexagonal titanium maintains a coherent interface with a tetragonal rutile through a sandwiched buffer zone of a TiO phase (rock salt). The angle between the ⟨1 1 0⟩ of TiO_2 and the ⟨0 0 0 1⟩ of Ti is about 43°. Based on Tanaka's work, an atomistic structure for a Ti/TiO_2/Cu interfacial area is schematically portrayed in Fig. 7. From an energetic viewpoint, an atomic layer of oxygen ions is assumed to cover the free TiO_2 surface. When deposited to the Ti/TiO_2 cathode, copper ions are also assumed to form a CuO (or possibly Cu_2O) layer before forming a copper crystallite. The CuO buffer zone is reasoned to promote coherency as well as compatibility between fcc Cu and TiO_2.

In the initial stage of electrodeposition at 65 °C, a defect-free rutile should be an ideal insulator with zero charge carriers because the Boltzmann probability with $E_g = 3$ eV is only 10^{-22}. This suggests that the electrons supplied to the cathode must transfer through the oxide layer via tunneling. Let us examine the transmission probability of the electrons through tunneling: according to the tunneling theory [2], the probability may be given by:

$$P = \exp\left[\frac{-4\pi l}{h}(2m\Delta E)^{1/2}\right] \quad (1)$$

where l is the oxide thickness, m the electron mass, h the Planck's constant and ΔE is the energy barrier for tunneling.

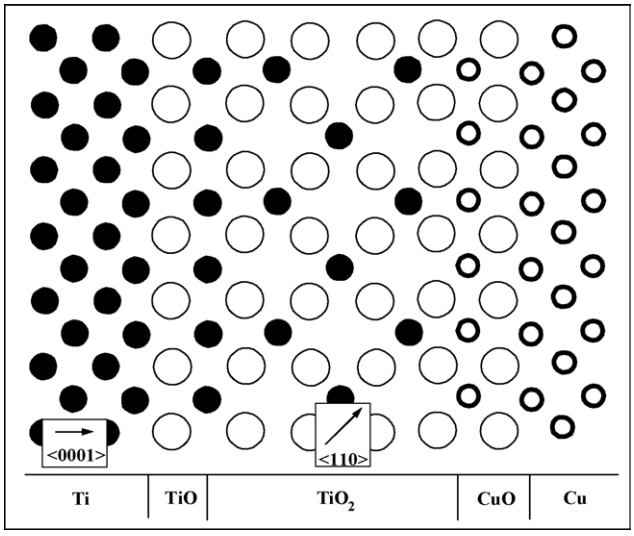

Fig. 7. A schematic for the atomistic structure of a $Ti/TiO_2/Cu$ interfacial area. Reasonable coherency between TiO_2 and Ti (or Cu) is viewed to maintain through a buffer zone of TiO (or CuO).

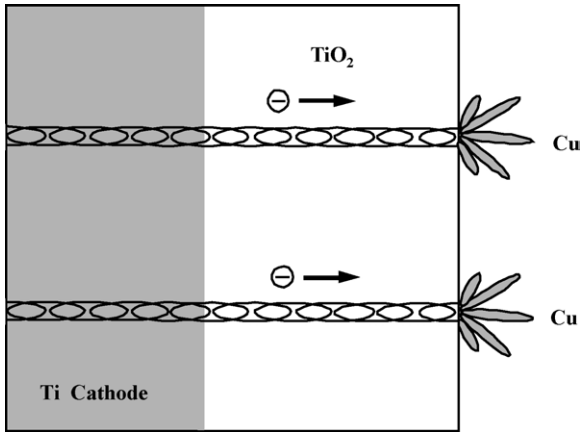

Fig. 8. A schematic for charge transfer in an oxide-covered titanium cathode via "pipe tunneling" mechanism along dislocation cores.

If we take 10^{-10} as the transmission probability for viable copper nucleation, the maximum oxide thickness is equal to 1.3 nm for $\Delta E = 3$ eV. That is, if ΔE is close to rutile's energy gap, only those oxide layers of 1.3 nm thick or less can become workable sites for copper nucleation. The band energy gap, E_g is taken as the upper bound for ΔE. Strictly speaking, ΔE is not equal to the oxide band energy gap, but should be close to the difference between the minimum energy level of the oxide conduction band and the Fermi level of titanium [17]. In view of the complex interface structure (see Fig. 7), the Fermi level of titanium is assumed to be the maximum energy level of the oxide valence band in this argument. If there arises some kind of electronic polarization, ΔE could be reduced to a lower value. For the probability to be 10^{-10} or greater [18], a 2 nm thick oxide layer requires $\Delta E \sim 1.27$ eV and only $\Delta E \sim 0.56$ eV for a 3 nm thick oxide layer. Although current understanding for the magnitude of a tunneling energy barrier is still sketchy at most, a recent theoretical investigation reports that molecular electronic polarization could enhance the transmission probability by an order of 100 [19]. This means only about a 10% decrease in ΔE, which is much shorter than the necessary 60–80% decrease for a 2–3 nm thick rutile film. Therefore, in view of the scratch experiments discussed above, 'pipe tunneling' along a dislocation core is proposed for copper nucleation, at least in the early stage of electrodeposition with a low current density.

In Fig. 8, a schematic is pictured for copper nucleation through pipe tunneling on an oxide-coated titanium substrate. Because of good coherency maintained between the substrate and the thin oxide layer of 2–3 nm thick, dislocations are pictured to be uninterrupted across the metal-oxide interface area. This view is consistent with the idea implicitly assumed in etch-pitting techniques to reveal dislocation positions [13,14]. If so, then what makes the dislocation cores within the oxide layer enhance charge transfer? Being imperfect, the energy states along a dislocation core should be different from those of the perfect lattice: thus there should be more acceptor- and donor-like charge traps in the vicinity of dislocations cores [20]. In addition to the structural imperfection related to the dislocation themselves, segregated impurities in the strain field of dislocations could also be responsible for the traps. Furthermore, because of deficiency in stoichiometry, a dislocation can be charged along its line: if so, a positively charged dislocation, for example, with extra Ti ions, will allow tunneling to occur more readily. Additionally, but perhaps more importantly, because of its strain field, the surface terminal of a dislocation line was attacked by the electrolyte, and in fact the terminal itself was already an etch-pit before the inception of electrodeposition. In brief, dislocations were considered to be a high electron tunneling path with a reduced energy barrier, ΔE, and a reduced barrier thickness, l in Eq. (1). Following the term, 'pipe diffusion' of solute atoms along a dislocation core, pipe tunneling of electrons along a dislocation line is coined. The energy barrier, $\Delta E \sim 0.56$ eV for a 3 nm thick oxide for a plausible pipe tunneling mechanism, seems reasonable in view of recent works on a single electron tunneling system, which suggests about 0.22 eV for semiconducting anatase TiO_2 [21].

3.3. Surface modification

To improve copper nucleation kinetics, i.e. to enhance charge transfer rates, cathode surface modification was attempted. One extreme measure would be to destroy the oxide layer exposing bare Ti surface to the electrolyte or alternately to coat the surface with another metal element. As described earlier, however, the oxide layer provides copper foil industry with an important beneficial effect, that is, an easy separation between the finished copper foil of 2–4 m wide but only 10–35 μm thick from the large cathode

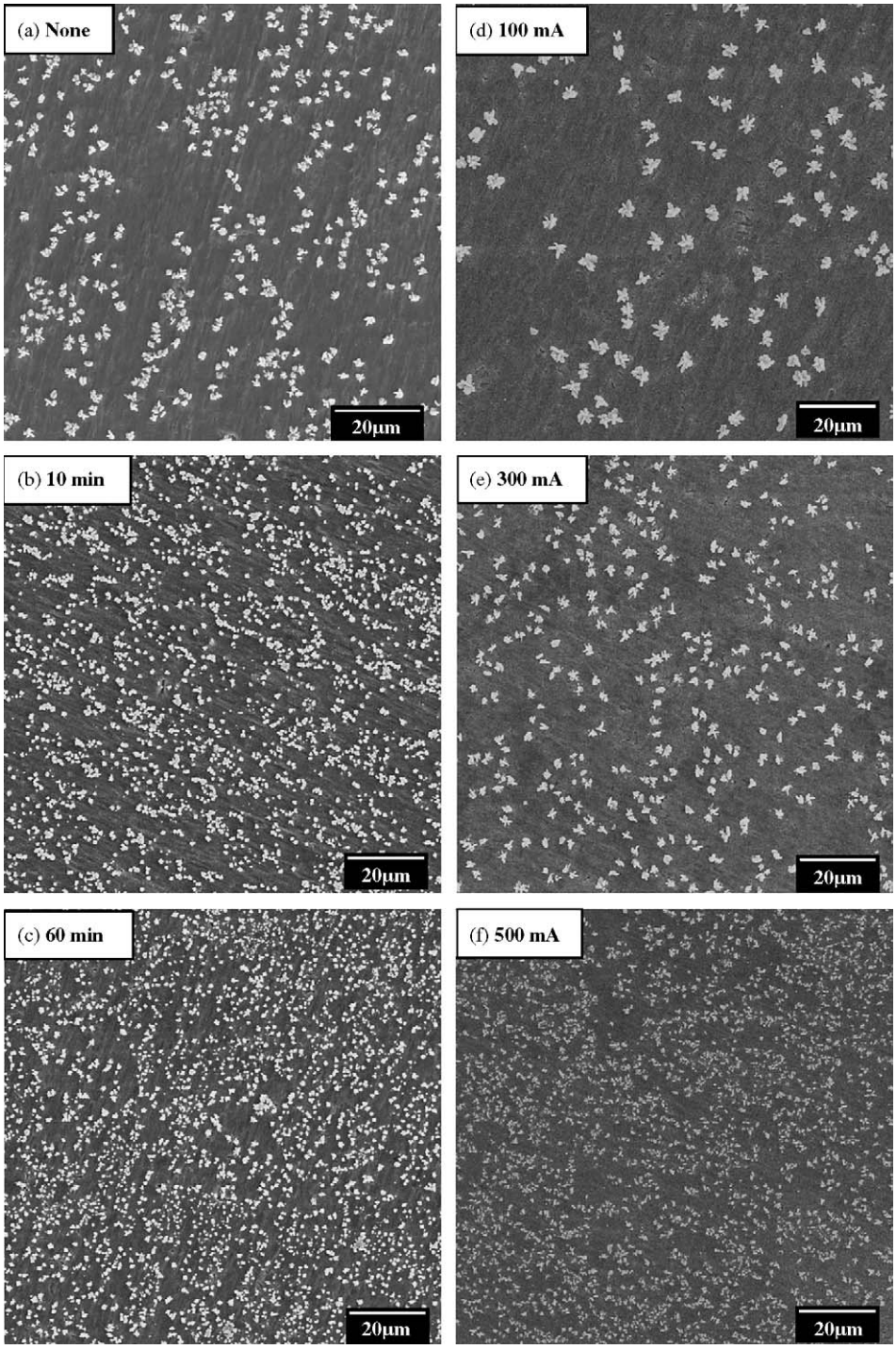

Fig. 9. Copper cluster distribution with different cathode surface treatments. (a) No surface treatment. (b and c) Are for the cathodes heat-treated at 400 °C for 10 and 60 min, respectively. (d–f) Are for the cathodes anodized for 1 s at 100, 300 and 500 mA/cm^2, respectively, prior to electrodeposition.

drum. Therefore, our efforts were focused on the modification of the oxide layer in two ways: (a) furnace oxidation and (b) anodization. In the furnace-oxidation approach, cathodes were heat-treated in a muffle furnace at 400 °C up to 1 h. In the anodization process, titanium cathodes were, prior to electrodeposition, anodized at 65 °C and at the current density of up to 1 A/cm^2 for 1 s.

In both cases, as shown in Fig. 9, finer and denser copper clusters were found when the surface was treated beyond a critical amount of either the oxidation time or the anodizing current. Fig. 9a shows a cluster distribution on an un-treated cathode surface after 1-s electrodeposition at a current density of 200 mA/cm^2. The images Fig. 9b and c are for the cathodes, which were heat-treated in an ambient air for 10

and 60 min, respectively. Clearly, the higher cluster density indicates that the cathode surface structure was modulated during the furnace heat-treatment. As pointed out by Teng et al. [22], the oxide films became thick but quite defective. The oxide films were estimated to be about 8 nm for the 10-min and 21 nm for the 60-min heat-treated ones. Consequently, the oxide structures were possibly not in the stable rutile form, but in other polymorphes such as anatase or brookite, which were defective with anion vacancies [22]. Another reason can be associated with an increase in the Pilling–Bedworth (PB) ratio [23], that is, the ratio of the oxide volume per Ti atom to the Ti atomic volume. The PB ratios are 1.77 for rutile, 1.82 for brookite and 1.90 for anatase. Therefore, higher coherency strain should have built up in either anatase or brookite films. As the elastic strain increased with an increase in epitaxy thickness, anatase (or brookite) films became increasingly conductive with ionic point defects generated intrinsically and/or extrinsically. With plenty of charge carriers, copper nucleation was more copious even though the films were thick.

When a titanium cathode surface was anodized, titanium dissolution could not be active since the electrode was nearly inert with the rutile film. Instead, dissolution of hydroxyl ions occurred, producing oxygen through reactions such as $4(OH)^{-1} = 2H_2O + O_2 + 4e^{-1}$. Some of the oxygen molecules nucleated gaseous bubbles. Some diffused through the oxide layer and reacted with the titanium atoms, consequently thickening the oxide layer. In fact, the color of the anodized cathode changed with an increase in the applied current density, indicating a variation in the film thickness as well as in the structure [24]. A spectrum of surface colors ranging from gold to blue and purple are displayed in Fig. 10. As

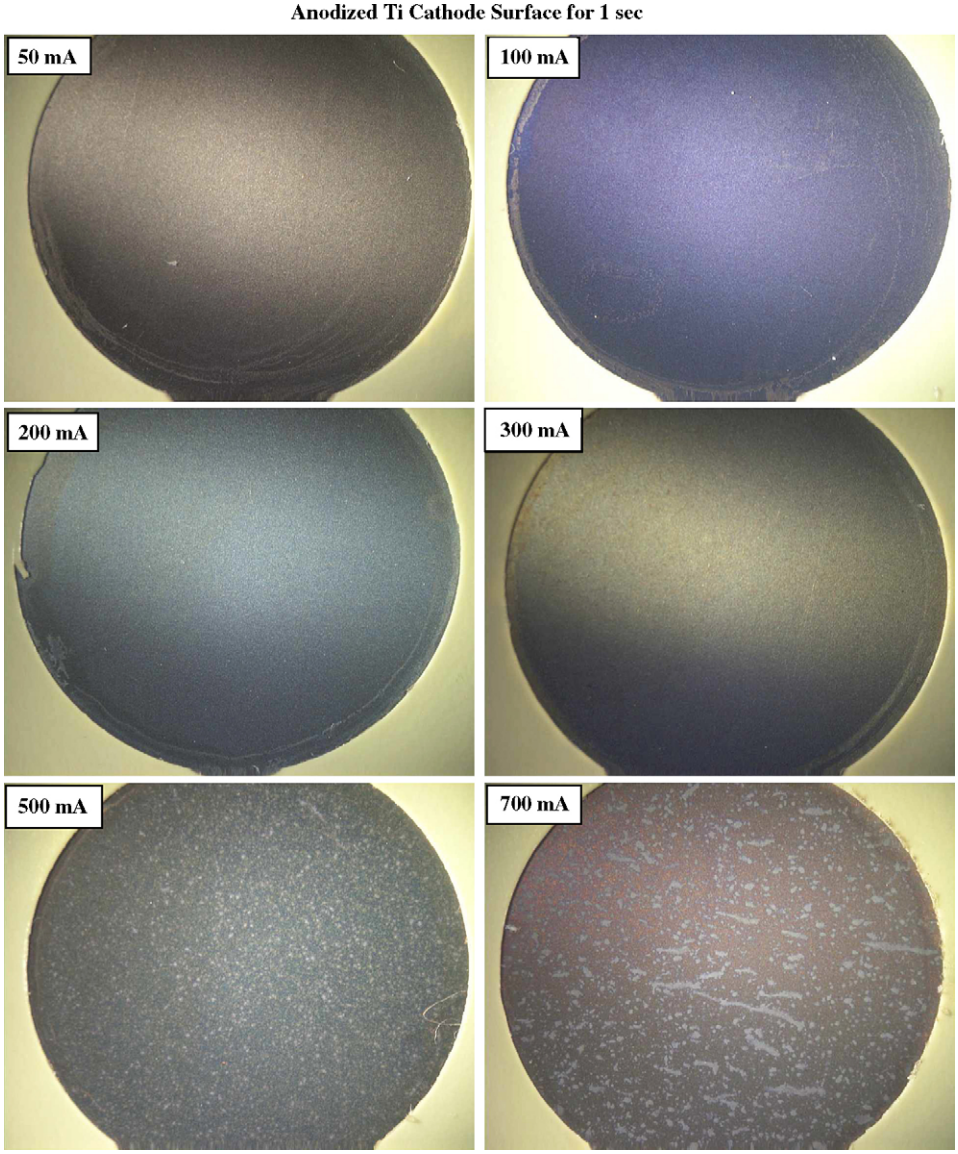

Fig. 10. A spectrum of titanium surface colors ranging from gold to blue and purple, which were anodized for 1 s at the currents from 50 to 700 mA/cm^2.

shown in Fig. 9d–f, the copper cluster density did not increase until the anodizing current density was over 300 mA/cm^2. A detailed study by Habazaki et al. [25] reported that in addition to the formation of anatase phase, amorphous titania was also produced during titanium anodization. The surface images at both 500 and 700 mA/cm^2 in Fig. 10 exhibit porous structures, suggesting numerous traces of gas bubbles and possibly amorphous phase. Based on the amount of charges passed during the anodization, the oxide thickness was estimated to be about 50–100 nm [24]. Clearly, anodized titanium cathode surfaces demonstrated enhanced copper nucleation rate through modified electronic structures.

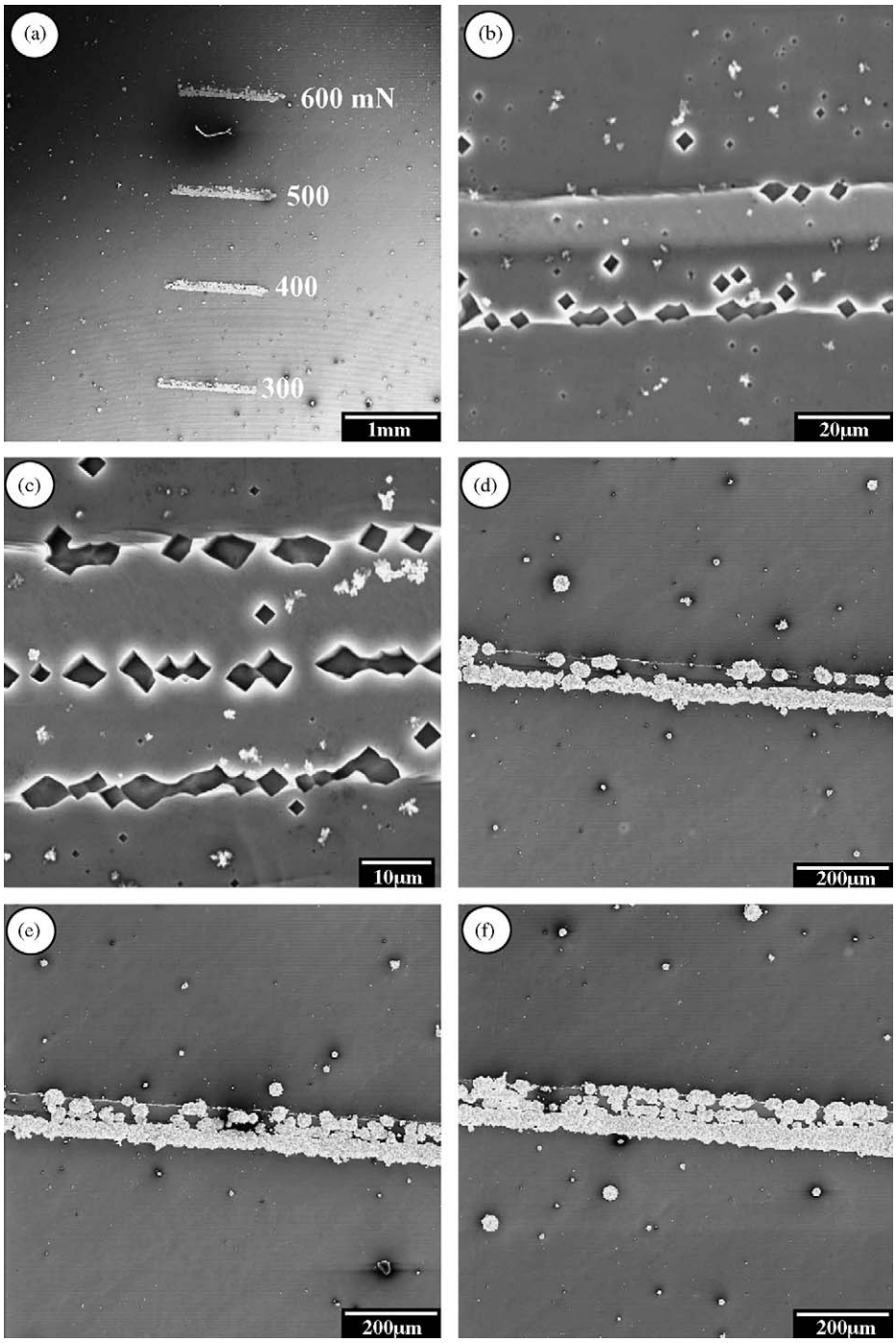

Fig. 11. Copper deposition on aluminum cathode surfaces. (a) Shows preferred copper deposition along scratch lines created under the loads of 300, 400, 500 and 600 mN. (b and c) Display etch-pits along the scratch lines created with 50 and 100 mN load. (d–f) Are for the cases with 200, 300 and 400 mN load, respectively.

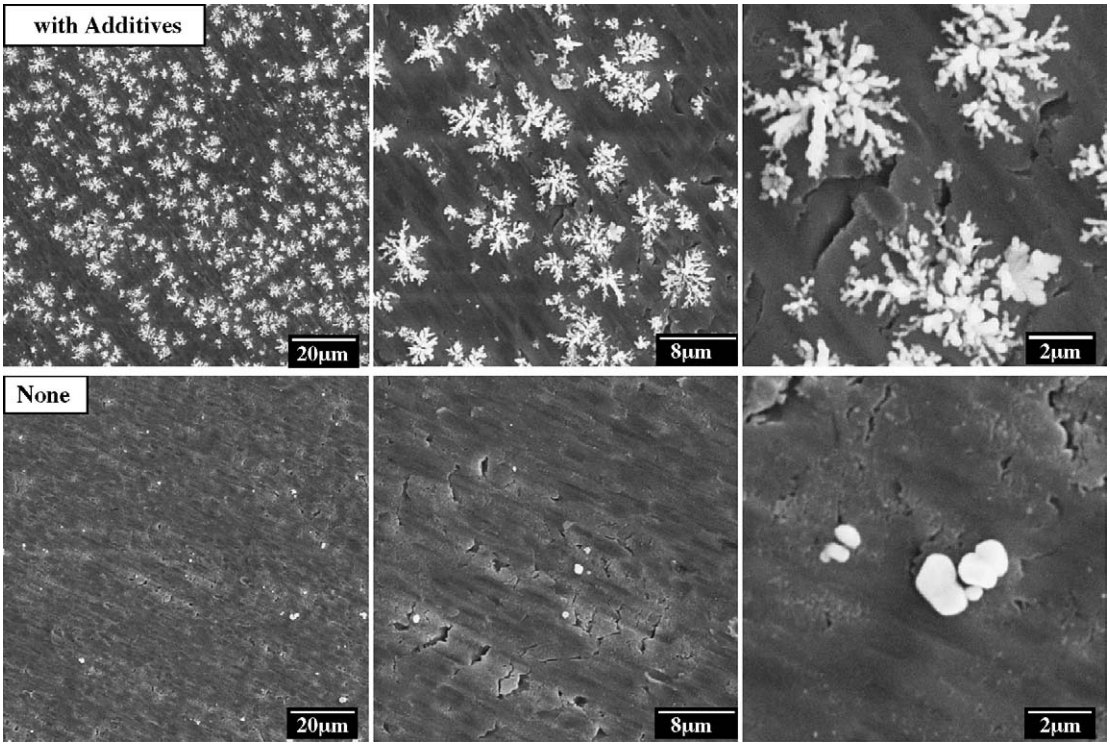

Fig. 12. The top row is for cluster images influenced by additives and the bottom images are those without additives under a pulsed potentiostatic condition. The additives were chlorine, glue and polyethylene imide as described in text.

4. Discussion

For ex situ scratched samples, etch-pitting techniques were attempted to reveal dislocations on the Ti cathode surface, but were unsuccessful due to lack of appropriate etching solutions. As an alternate, aluminum cathodes were investigated to locate dislocations both in the matrix region as well as along scratch lines. Fig. 11 displays copper clusters deposited on aluminum cathode surfaces with passive Al_2O_3 films. Fig. 11a shows preferred copper deposition along scratch lines created under the loads of 300, 400, 500 and 600 mN. The current density was fixed at 300 mA/cm^2 for 1 s. The aluminium cathodes were first electropolished, scratched with the nano-indenter, and then etched before electrodeposition. Both Fig. 11b and c exhibit etch-pits of typical diamond shapes along the scratch lines created with 50 and 100 mN, respectively. A few minute copper clusters are also noticeable. Copper nucleation appears to have preferred small and shallow pits due to the nature of charge distribution. With increasing scratch force, however, more dislocations should have been created, and the resulting effects are shown in Fig. 11d–f with 200, 300 and 400 mN load, respectively. With abundant dislocations, copper deposition became so active that neither etch-pits nor copper clusters were resolvable.

The micrograph of 500 mA/cm^2 of Fig. 1b advocates that copper nucleation was progressive, i.e. new clusters emerged continuously in time. At first, this appears contradictory to the pipe tunneling mechanism, but is not. A higher current requires a higher cathode potential (~ -1 eV at 500 mA), hence a higher overpotential for discharging copper ions. With an increased cathode potential, the tunneling energy barrier, ΔE, should decrease (due to a higher Fermi level in Ti), resulting in a higher probability over the oxide film. It should also be noted that when copper ions began to deposit on the substrate surface, they were essentially forming new "oxides" (in the form of Cu_2O or CuO) with the oxygen ions on the surface layer of TiO_2 (see Fig. 7). This new oxidation process may change the dielectricity of the rutile film with newly created point defects or energy states, again improving the conductivity. It may be safe further to say that the "copper oxide" (at least the first monolayer) spreads kind of chain nucleation in its neighborhood, as oxidation creates coherency strain. Put it in terms of classical nucleation theory, the neighborhood of a copper cluster now becomes ripe for nucleation with a lower activation energy—sympathetic nucleation [26]. Even with a low current like 200 mA/cm^2, there was an indication of progressive mode at a longer deposition time, and it can be viewed as a sympathetic nucleation phenomenon.

Another way to modify electrodeposition kinetics is to dissolve minute amounts of organic and/or inorganic additives into the electrolyte. In fact, various additives are widely practiced in copper foil industry, and numerous investigations were attempted to understand their beneficial mechanisms, which still remain unresolved [1–3]. As an example, Fig. 12 shows deposition results performed under a pulsed potentio-

static condition, in which the applied potential was cycled between −1.7 and −0.4 V with a time interval of 0.02 s for 50 cycles. The top row presents cluster images influenced by additives, which are compared to those without additives in the bottom. The additives were chlorine (20 mg/l), glue (2 mg/l) and polyethylene imide (PEI) (2 mg/l). Clearly, the influence of the additives was profound as compared to the additive-free case. Without the additives, cluster nucleation was sparse and the few clusters grew almost equiaxed or round. With the additives, however, copper clusters appear to have displayed a two-dimensional fractal growth through diffusion limited aggregation on the cathode surface. It seemed that before reduced to become lattice atoms, cuprous copper ions were forced to sustain active surface diffusion under the combined influence of PEI and chloride ions. Chloride ions are known to promote one-dimensional crystal growth, whereas PEI is suspected to influence a leveling effect through the interaction between its nitro-aromatic group and copper ions. Apparently, under a pulsed potentiostatic condition, the synergetic effect between PEI and chloride ions promoted crystal growth limited by surface diffusion of copper ions on the cathode surface. Glue, made of various polypeptides containing amino acids, was found to play a role less effective than PEI. Without question, further detailed studies are needed to understand the role of additives as well as the effect of pulsed charging on nucleation and growth of copper clusters.

5. Conclusion

Copper nucleation kinetics during electrodeposition with Ti cathodes was investigated. Because of the stable rutile oxide film with a large band energy gap, pipe tunneling mechanism for electron transfer along a dislocation core was proposed to account for the enhanced nucleation rate, at least in the early stage of electrodeposition at low current densities. Both ‘in situ’ and ‘ex situ’ scratch tests were demonstrated to support the pipe tunneling mechanism. In order to improve the conductivity of the oxide film, the Ti cathode surface was modified through furnace oxidation and anodization process. Both cases showed enhanced nucleation kinetics as the oxide structure became more conductive in spite of its increased thickness.

Acknowledgments

The financial support by L.G. Cable of Korea through Michigan Technological University is greatly appreciated. J.K.L. was honoured to present this work at the special symposium dedicated to Professor James C.M. Li on his 80th birthday.

References

[1] J.O’M. Bockris, A.K.N. Reddy, Modern Electrochemistry, vol. 1–2, Plenum Press, New York, 1970.
[2] J.O’M. Bockris, A.K.N. Reddy, M. Gamboa-Aldeco, Modern Electrochemistry, vol. 2A, second ed., Kluwer Academic, New York, 2000.
[3] M. Schlesinger, M. Paunovac, Modern Electorplating, fourth ed., Wiley, New York, 2000.
[4] J.H. Choi, S.Y. Kang, D.N. Lee, J. Mater. Sci. 35 (2000) 4055.
[5] B.-Z. Lee, D.N. Lee, Acta Mater. 46 (1998) 3701.
[6] W.P. Lorenz, T.J. O’Keefe, C.B. Sonnio, Surf. Technol. 6 (1978) 179.
[7] J.B. Dutra, T.J. O’Keefe, in: J.E. Dutrizac, al. et (Eds.), Proceedings of Copper 99-Cobre 99 International Symposium, vol. III, TMS, Warrendale, 1999, p. 495.
[8] K.-W. Seol, B.-H. Choe, Y.-K. Lee, J.K. Lee, Mater. Sci. Forum 426–432 (2003) 3715.
[9] B.H. Choe, K.W. Seol, J.A. Jeannette, A.D. LaLonde, J.K. Lee, in: W.E. Frazer, et al. (Eds.), LiMAT-2003, Postech, Korea, 2004, p. 237.
[10] B. Grosgogeat, L. Reclaru, M. Lissac, F. Dalard, Biomaterials 20 (1999) 933.
[11] K. Rohly, N. Istephanous, A. Belu, D. Untereker, M. Cosco, J. Heffelfinger, R. Thomas, J. Allen, R. Francis, A. Robinson, N. Perron, B. Sahli, B. Kobielush, Mater. Sci. Forum 426–432 (2003) 3017.
[12] V.H. Bulsara, S. Chandrasekar, T.N. Farris, ASM Handbook, vol. 8, ASM International, 2000, p. 317.
[13] D.F. Stein, J.R. Low Jr., J. Appl. Phys. 31 (1960) 862.
[14] H.W. Schadler, Acta Metall. 12 (1964) 861.
[15] G.S. Rohrer, Structure and Bonding in Crystalline Materials, Cambridge, Cambridge, 2001.
[16] Y. Tanaka, http://dent.sympo.nagasaki-u.ac.jp/baylor/tanaka/presentation.html.
[17] M. Lenzlinger, E.H. Snow, J. Appl. Phys. 40 (1969) 278.
[18] F. Rana, S. Tiwari, D.A. Buchanan, Appl. Phys. Lett. 69 (1996) 1104.
[19] A. Mosyak, P. Graf, I. Benjamin, A. Nitzan, J. Phys. Chem. 101A (1997) 429.
[20] E.G. Brazel, M.A. Chin, V. Narayanamurti, Appl. Phys. Lett. 74 (1999) 2367.
[21] K. Matsumoto, M. Ishii, K. Segawa, Y. Oka, B.J. Vartarnian, J.S. Harris, Appl. Phys. Lett. 68 (1996) 34.
[22] K.S. Teng, J.-L. Delplancke, J. Zhang, T.J. O’Keefe, Metall. Mater. Trans. 29B (1998) 749.
[23] D.R. Askeland, The Science and Engineering of Materials, PWS, Boston, 1994.
[24] J.-L. Delplancke, M. Sun, T.J. O’Keefe, R. Winand, Hydrometallurgy 23 (1989) 47.
[25] H. Habazaki, M. Uozumi, H. Konnon, K. Shimizu, J. Corros. Sci. Eng. 6 (2004) 107.
[26] H.I. Aaronson, J.K. Lee, K.C. Russell, in: K.C. Russell, H.I. Aaronson (Eds.), Precipitation Processes in Solids, TMS, Warrendale, 1978, p. 31.